IEEE Access
Multidisciplinary | Rapid Review | Open Access Journal

Received June 24, 2019, accepted July 4, 2019, date of publication July 11, 2019, date of current version July 29, 2019.

Digital Object Identifier 10.1109/ACCESS.2019.2928004

Cooperative Adaptive Cruise Control With Adaptive Kalman Filter Subject to Temporary Communication Loss

CHAOXIAN WU[1,2], YUAN LIN[2], (Member, IEEE), AND AZIM ESKANDARIAN[2], (Senior Member, IEEE)

[1]Hubei Key Laboratory of Advanced Technology for Automotive Components Automobile Engineering Institute, Wuhan University of Technology, Wuhan 430000, China

[2]Department of Mechanical Engineering, Virginia Tech, Blacksburg, VA 24060, USA

Corresponding author: Chaoxian Wu (cxw@vt.edu)

The work of C. Wu was supported by the China Scholarship Council for him to conduct this research as a visiting doctoral student in Autonomous Systems and Intelligent Machines Lab of the Department of Mechanical Engineering of Virginia Tech, Blacksburg, VA 24060 USA.

ABSTRACT Cooperative adaptive cruise control (CACC) communicates the relevant preceding vehicle state data to the follower (ego) vehicle to improve the vehicle following capabilities. In general, the CACC utilizes the preceding vehicle's desired acceleration from wireless communication as a feedforward term in the controller of the ego vehicle, which dominantly determines the total control input. However, communication loss would degrade CACC to adaptive cruise control (ACC), where the lack of the feedforward term during communication loss would increase the inter-vehicular distance or, otherwise, may lead to collision during vehicle emergency braking. This paper proposes a control algorithm with an adaptive Kalman filter estimating the acceleration of a preceding vehicle, and the estimated acceleration is implemented as a feedforward signal in the ego-vehicle CACC controller in case of communication loss. The proposed control algorithm is evaluated by the experiments using mobile robots that emulate driving. In addition, the simulations of real vehicles are also conducted. The results of simulations and robot experiments show that the performance of implementing the adaptive Kalman filter during communication loss is better than fallback to ACC and the normal Kalman filter based on the Singer model.

INDEX TERMS Communication loss, adaptive Kalman filter, statistical model, cooperative adaptive cruise control (CACC), acceleration estimation.

I. INTRODUCTION

Cooperative adaptive cruise control (CACC) achieves the vehicle longitudinal automation, by utilizing the inter-vehicle distance mostly from radar and the vehicle state information received from wireless communication [1], to improve safety, fuel economy and traffic throughput [2]. For safety improvement, CACC is able to reduce the diversity of vehicles' behavior in traffic, which is one of the main reasons for vehicle crashes [3]. The fuel consumption can also be reduced by more than one-third by implementing CACC in a signalized corridor [4]. In the perspective of traffic throughput, a 100 percent deployment of CACC can increase the traffic throughput from 2000 veh/hr/ln in manual driving to 4200 veh/hr/ln [2]. All of these are possible because CACC allows shorter and smoother safe gaps between vehicles.

The associate editor coordinating the review of this manuscript and approving it for publication was Heng Zhang.

CACC is able to perform vehicle following with smaller inter-vehicle distance and maintain the string stability, compared with adaptive cruise control (ACC) [5]. The most common information flow topology is the predecessor following CACC, in which the preceding vehicle sends its desired acceleration to the following vehicle [6]–[8]. The preceding vehicle's desired acceleration is implemented as the feedforward term in CACC controller of the ego vehicle and dominantly determines the total control action, especially during transient behavior [7], [9], [10]. For example, in PD-controllers, the feedforward term in CACC controller determines up to 80% of the total control action [7]. Hence, the preceding vehicle's desired acceleration is extremely important in CACC controller.

However, communication impairments, such as communication loss [10]–[12], latency [13], [14] and security problem [15]–[17], can compromise the performance of CACC. The study of communication loss in CACC attracts lots of

attention in recent years. There are two kinds of communication loss scenarios in CACC, including the random communication loss in a short period and the extended communication loss in an extended period. To address the random communication loss in a short period, many researchers implemented the consensus-based controller to utilize the surrounding vehicle state information from the rest of available communication links [18]–[20]. In the extended communication loss scenario, the CACC controller cannot receive the preceding vehicle's desired acceleration, and it has to degrade to ACC for ensuring vehicle safety. Hence, it is necessary to improve the CACC controller performance during the extended communication loss period. This paper mainly focuses on analyzing the extended communication loss problem in the homogeneous platoon. Previously, three kinds of solutions have been proposed to deal with the extended communication loss. The first one is fallback to ACC. When communication loss happens, CACC normally falls back to ACC for maintaining string stability, which enlarges the inter-vehicle distance and degrades its performance [21]. The second one is to use a better wireless communication protocol. Lee, K.K. and Chanson, S.T. proposed a wireless communication protocol, in which a lost packet was resent until it exceeded the requirement of maximum time delay [22]. This method induces high communication delay, which might compromise the string stability of CACC [23]. The third one is proposing an advanced CACC control algorithm. Nunen, E.v., et al proposed a model predicted control (MPC) for CACC, in which vehicles shared their own predictions of the desired acceleration in MPC controller through wireless communication and the following vehicle saved this information of the preceding vehicle [10]. The following vehicle utilizes this saved information as a feedforward signal in CACC controller when communication loss happens. However, this method is effective only when the communication loss is within the prediction horizon of the MPC controller, usually within 1 second [24]. Another research [11] proposed a dynamic spacing policy during communication loss, which had a risk of collision during vehicle braking. Ploeg, J., et al utilized the estimated preceding vehicle's acceleration as a feedforward term in CACC controller during communication loss [12]. This method can be implemented for a few seconds during communication loss. Hence, compared to above methods, the estimation of the preceding vehicle's acceleration is a better solution to improve the inter-vehicle distance tracking performance of CACC in case of extended communication loss.

Kalman filter is widely implemented to estimate the states of maneuvering targets (ego-vehicle or other vehicles) due to its high computational efficiency. In case of unknown control action of maneuvering targets, there are many linear motion models which can be utilized to design a Kalman filter for maneuvering target states estimation. Among them, white noise models and Markov process models are mostly utilized [25]. On one hand, white noise models, like the constant velocity model and the constant acceleration model, model the control action of the target as white noise, which is easy to implement. The constant acceleration model was employed to estimate the states of ego-vehicle [26] and other vehicles [27]. However, the actual control action of the target rarely has a constant acceleration. On the other hand, Markov process models, like the Singer model and the ''current'' model, regard the control action of the target as a Markov process model, in which the control action of the target has time correlation. The Singer model was employed to estimate the preceding vehicle's acceleration, which is used to improve the inter-vehicle distance tracking performance of CACC during communication loss [12]. The Singer model assumes the probability density function (PDF) of acceleration is a symmetric ternary-uniform mixture distribution with zero mean. However, the Singer model does not utilize the past estimated acceleration information to estimate the new value [25]. And the ''current'' model utilizes the estimated acceleration in the last step as the new acceleration mean and assumes a conditional PDF with this new acceleration mean, which improves the accuracy of state estimation [28]. Hence, the ''current'' model has better acceleration estimation accuracy than the Singer model.

This paper proposes an innovative CACC control strategy with an adaptive Kalman filter and a calculation method of the measurement vector of the preceding vehicle. Compared to the acceleration estimation method in [12], on one hand, the ''current'' model is utilized to build the adaptive Kalman filter in this paper instead of the normal Kalman filter based on the Singer model in [12]. Based on the analysis in the last paragraph, the ''current'' model can provide a better acceleration estimation accuracy than the Singer model. On the other hand, the calculation method of the measurement vector of the preceding vehicle in [12] includes the inter-vehicle distance, the relative velocity, and the longitudinal acceleration, in which the longitudinal acceleration is from the accelerometer. The measured signal from an accelerometer could increase the oscillation of the estimated acceleration. Hence, this paper proposed a new calculation method of the measurement vector of the preceding vehicle, which is based on the inter-vehicle distance, the relative velocity, the self-velocity, and the self-position. This calculation method can avoid the oscillatory feedforward control input. The assumptions and methods for measuring or estimating each of these variables are specified in Section III-A and B where the controller is introduced. This approach provides a better proceeding vehicle state estimation for the control of the follower (ego) vehicle. The results presented herein reflect this improvement.

The rest of this paper is organized as below. Section II illustrates the vehicle longitudinal dynamic model for simulations and the CACC control strategy without communication loss. Section III presents the proposed control strategy with the adaptive Kalman filter and the calculation of the measurement vector. Section IV presents the results of simulations and experiments. Section V draws conclusions and future work.

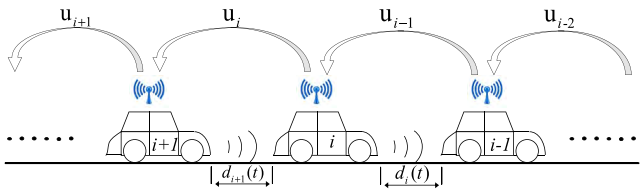

FIGURE 1. Predecessor following CACC.

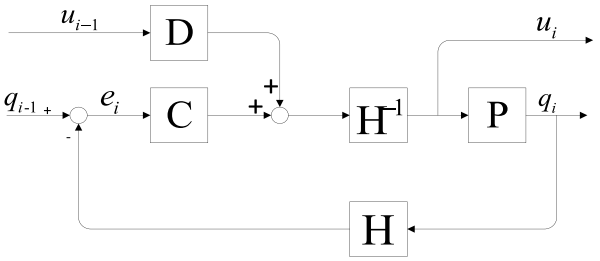

FIGURE 2. Control block diagram of CACC.

II. VEHICLE MODEL AND CACC CONTROLLER

A. VEHICLE LONGITUDINAL DYNAMICS MODEL

The transfer function below is utilized to model the longitudinal dynamic for every vehicle in the CACC platoon, which considers the actuation delay ($\tau_{a,i}$) [7], [29]. This vehicle longitudinal model is widely used for platoon performance evaluation [30].

$$P_i(s) = \frac{q_i(s)}{u_i(s)} = \frac{1}{s^2(\eta_i s + 1)} e^{-\tau_{a,i} s} \tag{1}$$

wherein $q_i(s)$ is the absolute position of vehicle i in the Laplace domain, $u_i(s)$ is the desired acceleration of vehicle i in the Laplace domain, η_i is a vehicle actuator dynamic parameter of vehicle i, and $P_i(s)$ is the plant of vehicle i.

B. CACC CONTROLLER

The CACC controller is to keep a desired inter-vehicle distance between vehicles while maintaining the string stability. CACC algorithms could assume different communications topologies by utilizing the state of one vehicle ahead or multiple vehicles around. The predecessor following CACC platoon adopted in this research is illustrated by Fig. 1.

The desired inter-vehicle distance is calculated by a constant time gap strategy, as shown below.

$$d_{r,i}(t) = r_i + h v_i(t) \tag{2}$$

wherein $d_{r,i}(t)$ is the desired inter-vehicle distance of vehicle i; r_i is the standstill distance of vehicle i; $v_i(t)$ is the velocity of the vehicle i; and h is the time gap. Hence, the control error is

$$e_i(t) = d_i(t) - d_{r,i}(t) \tag{3}$$

wherein $d_i(t)$ is the actual inter-vehicle distance of vehicle i; and $e_i(t)$ is the control error of vehicle i.

To regulate this error, a CACC controller implementing predecessor following communication topology is employed (see Fig. 2), which is a PD controller with a feedforward signal [31]. The CACC controller in the Laplace domain is presented below [7]. A pre-compensator $H^{-1}(s)$ is designed to cancel the effect of $H(s)$ in the control feedback loop, such that the time gap h can be set to any value without retuning other control gains in the loop.

$$u_i(s) = H^{-1}(s)(k_p e_i(s) + k_d s e_i(s) + u_{i-1}) \tag{4}$$

$$H(s) = hs + 1 \tag{5}$$

$$C(s) = k_p + k_d s \tag{6}$$

$$D(s) = e^{-\theta s} \tag{7}$$

wherein k_p and k_d are the PD controller coefficients; $H(s)$ is the transfer function related to the desired inter-vehicle distance policy (2); $C(s)$ is the PD controller of vehicle i; $D(s)$ is the wireless communication delay; and θ is the wireless communication time delay constant.

III. ADAPTIVE KALMAN FILTER

To prevent a substantial degradation when communication fails for an extended period (within a few seconds), an adaptive Kalman filter, utilizing the "current" model as motion model, is implemented to estimate the preceding vehicle's acceleration, such that the estimated acceleration can be utilized as a feedforward signal in case of communication loss. In the remainder of the paper, the CACC controller with the adaptive Kalman filter or the normal Kalman filter means the CACC controller of the ego vehicle utilized the estimated acceleration of the preceding vehicle, calculated by the adaptive Kalman filter or the normal Kalman filter, as the feedforward term during communication loss. Fallback to ACC means the CACC controller does not utilize any feedforward term during communication loss. Perfect CACC means there is no communication loss during the whole process.

Section III-A introduces the adaptive Kalman filter based on the "current" model and its difference from the normal Kalman filter based on the Singer model. Section III-B presents the calculation method of the measurement vector of a preceding vehicle. Section III-C introduces the discretization of the adaptive Kalman filter and the normal Kalman filter, which can be employed in the mobile robots for experimental validations [32].

A. THE "CURRENT" MODEL AND THE SINGER MODEL

The motion model in the adaptive Kalman filter is the "current" model. In contrast, the Singer model is the motion model of the normal Kalman filter. The state equation of the "current" model, proposed by [28], is illustrated below.

$$\begin{aligned}\dot{x}(t) &= \begin{pmatrix} \dot{q}(t) \\ \dot{v}(t) \\ \dot{a}(t) \end{pmatrix} = Ax(t) + B\bar{a}(t) + Gw(t) \\ &= \begin{pmatrix} 0 & 1 & 0 \\ 0 & 0 & 1 \\ 0 & 0 & -\alpha \end{pmatrix} \begin{pmatrix} q(t) \\ v(t) \\ a(t) \end{pmatrix} + \begin{pmatrix} 0 \\ 0 \\ \alpha \end{pmatrix} \bar{a}(t) + \begin{pmatrix} 0 \\ 0 \\ 1 \end{pmatrix} w(t)\end{aligned} \tag{8}$$

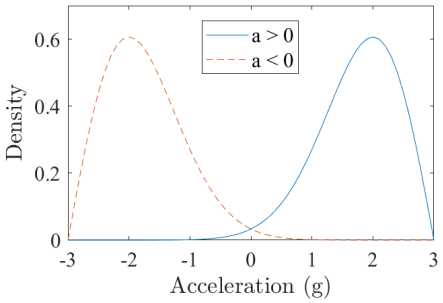

FIGURE 3. Conditional Rayleigh density ($c_k = 1$).

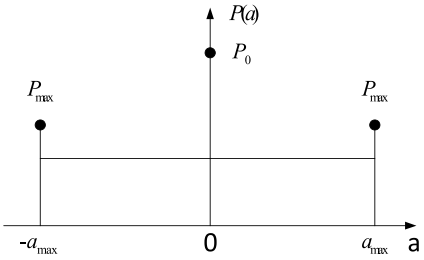

FIGURE 4. Symmetric ternary-uniform mixture distribution (P_0 is the probability of zero acceleration; and P_{max} is the probability of maximum acceleration.).

wherein $a(t)$, $v(t)$, $q(t)$ are the acceleration, velocity, and absolute position of the target, respectively; α is the maneuvering frequency; and $w(t)$ is the zero-mean process white noise, whose covariance matrix is Q.

The main difference between the ''current'' model and the Singer model is that the ''current'' model has an adaptive acceleration mean $\bar{a}(t)$, which will be updated continuously. However, the Singer model has the same state space equation with $\bar{a}(t) = 0$ [33].

The adaptive acceleration mean in the ''current'' model means utilizing the past estimated acceleration as the new acceleration mean, which can improve the acceleration estimation accuracy. And the adaptive acceleration mean $\bar{a}(t)$ is updated by the following equation during the estimation process.

$$\bar{a}_{k+1} = E[a_{k+1}|z^k] = E[a_k|z^k] = \hat{a}_k \tag{9}$$

wherein z^k is all the past measurements; and $\hat{a}_k$ is the acceleration estimation value at the time$k$.

To employ the adaptive Kalman filter or the normal Kalman filter, the process noise covariance matrix Q needs to be computed by the probability density function (PDF) of target acceleration. The PDF of the target acceleration in the ''current'' model is a conditional PDF $f(a|\hat{a}_k)$, which is a conditional Rayleigh density [28], as shown in Fig. 3. However, the PDF of target acceleration in the Singer model is an unconditional PDF, which is a symmetric ternary-uniform mixture distribution, as shown in Fig. 4.

The PDF of target acceleration in the ''current'' model is shown below.

$$f(a_{k+1}|\hat{a}_k) = \begin{cases} c_k^{-2}(a_{\max} - a)\exp(-(a_{\max} - a)^2/2/c_k^2) \\ \qquad l(a_{\max} - a) \quad \hat{a}_k \geq 0 \\ c_k^{-2}(a - a_{-\max})\exp(-(a - a_{-\max})^2/2/c_k^2) \\ \qquad l(a - a_{-\max}) \quad \hat{a}_k < 0 \end{cases} \tag{10}$$

wherein $l()$ is the unit step function; $a_{\max}$ and $a_{-\max}$ is the maximum acceleration and deceleration, respectively; and c_k is a $\hat{a}_k$ dependent parameter.

According to these PDFs, the variances of process noise in the ''current'' model and the Singer model are calculated by the first equation and the second equation below, respectively [25]. Also, it is assumed that $a_{\max} = a_{-\max}$.

$$\sigma_k^2 = \begin{cases} \dfrac{4-\pi}{\pi}(a_{\max} - \hat{a}_k)^2 & \hat{a}_k \geq 0 \\ \dfrac{4-\pi}{\pi}(a_{-\max} + \hat{a}_k)^2 & \hat{a}_k < 0 \end{cases} \tag{11}$$

$$\sigma_k^2 = \frac{a_{\max}^2}{3}(1 + 4P_{\max} - P_0) \tag{12}$$

wherein σ_k^2 is the variance of process noise.

The adaptive Kalman filter is built by combining equation (8) and the following equation for estimating the preceding vehicle's acceleration. The normal Kalman filter based on the Singer model is also built by equation (8) with $\bar{a}(t) = 0$ and the following equation.

$$y(t) = Cx + v(t) = \begin{pmatrix} 1 & 0 & 0 \\ 0 & 1 & 0 \end{pmatrix} x(t) + v(t) \tag{13}$$

wherein $v(t)$ is the measurement noise; and $y(t)$ is the measurement vector. The covariance matrix of measurement noise R is equal to $E(v(t)v^T(t))$, which is determined by the radar sensor characteristics. And the covariance matrix of process noise Q is calculated by the following equation.

$$Q = GE(w(t)w^T(t))G^T = \begin{pmatrix} 0 & 0 & 0 \\ 0 & 0 & 0 \\ 0 & 0 & 2\alpha\sigma_k^2 \end{pmatrix} \tag{14}$$

The estimated state of the adaptive Kalman filter and the normal Kalman filter are calculated by the following equation [34]. But, in the normal Kalman filter based on the Singer model, $\bar{a}(t) = 0$.

$$\dot{\hat{x}}(t) = A\hat{x}(t) + B\bar{a}(t) + L(y(t) - C\hat{x}(t)) \tag{15}$$

wherein $\hat{x}(t)$ is the estimated state of the target vehicle; L is the Kalman gain in Kalman filter. According to $w(t) \sim (0, Q)$ and $v(t) \sim (0, R)$, the Kalman gain L is attained by solving the corresponding error covariance algebraic Riccati equation, as demonstrated by the following equations. The Kalman gain in the normal Kalman filter is a constant due to the constant process noise covariance matrix Q in the Singer model. However, According to (11) and (14), the process noise covariance matrix Q in the adaptive Kalman filter is updating at each sampling period. Hence, the Kalman

gain in the adaptive Kalman filter needs to be recalculated at each sampling period.

$$AP + PA^T + GQG^T - PC^T R^{-1} CP = 0 \tag{16}$$
$$L = PC^T R^{-1} \tag{17}$$

B. CALCULATION OF MEASUREMENT VECTOR

The measurement vector of the preceding vehicle in the adaptive Kalman filter and the normal Kalman filter need to be modified for its calculations in CACC controller since the ego vehicle cannot measure the velocity and absolute position of the preceding vehicle. Based on the fact that the radar sensor installed in the ego vehicle measures the inter-vehicle distance and the relative velocity between the ego vehicle and the preceding vehicle, the measurement vector is modified as below.

$$y(t) = \begin{pmatrix} q_{i-1}(t) \\ v_{i-1}(t) \end{pmatrix} = \begin{pmatrix} q_i(t) \\ v_i(t) \end{pmatrix} + \begin{pmatrix} q_i(t) \\ v_i(t) \end{pmatrix} \tag{18}$$

wherein $v_i(t)$ and $q_i(t)$ are the relative velocity and the inter-vehicle distance between vehicle i and vehicle $i-1$, which is measured by the radar installed in vehicle i. Also, it is assumed that the velocity and position of the ego vehicle are measured or estimated precisely. This assumption is reasonable. For the measurement or estimation of vehicle velocity, the vehicle velocity can be measured precisely, by the wheel-speed sensor mounted on the non-driving wheel, except during the braking process. And the vehicle velocity also can be estimated by the wheel speed sensor and the longitudinal vehicle acceleration sensor [35]. For the measurement and estimation of vehicle position, the fusion of global navigation satellite systems and vehicle acceleration sensor or simultaneous localization and mapping (SLAM) can provide an accurate estimation or measurement of vehicle position [36]–[38]. Hence, the measurement vector is calculated by the measurement from radar and the estimation or measurement of vehicle position and velocity.

C. THE DISCRETIZATION OF THE ADAPTIVE KALMAN FILTER AND THE NORMAL KALMAN FILTER

The discretization of the adaptive Kalman filter and the normal Kalman filter need to be accomplished for their implementation in the digital controller. The discrete state space representation of the adaptive Kalman filter can be written as below [39].

$$X(k+1) = \Phi(k)X(k) + U(k)\bar{a}(k) + W(k) \tag{19}$$
$$Z(k) = H(k)X(k) + V(k) \tag{20}$$

wherein $\mathrm{X}(k) = (\, q(k)\ v(k)\ a(k)\,)^T$ is the state space vector; $a(k)$, $v(k)$, $q(k)$ are the acceleration, velocity and absolute position of the target at time k, respectively; $Z(k)$ is the measurement vector; $\Phi(k)$ is the state transition matrix; $H(k)$ is the measurement matrix; $W(k)$ and $V(k)$ are the process noise and the measurement noise with covariance matrix $Q(k)$ and $R(k)$, respectively; $U(k)$ is the input matrix; and $\bar{a}(k)$ is the adaptive acceleration mean.

The equations of $\Phi(k)$, $U(k)$, $Q(k)$ and $H(k)$ are shown as follows [40]:

$$\Phi(k) = \begin{pmatrix} 1 & T & (-1+\alpha T + e^{-\alpha T})/\alpha^2 \\ 0 & 1 & (1-e^{-\alpha T})/\alpha \\ 0 & 0 & e^{-\alpha T} \end{pmatrix} \tag{21}$$

$$U(k) = \begin{pmatrix} -T/\alpha + T^2/2 + (1-e^{-\alpha T})/\alpha^2 \\ T - (1-e^{-\alpha T})/\alpha \\ 1 - e^{-\alpha T} \end{pmatrix} \tag{22}$$

$$H(k) = \begin{pmatrix} 1 & 0 & 0 \\ 0 & 1 & 0 \end{pmatrix} \tag{23}$$

$$Q(k) = 2\alpha\sigma_k^2 \begin{pmatrix} q_{11} & q_{12} & q_{13} \\ q_{12} & q_{22} & q_{23} \\ q_{13} & q_{23} & q_{33} \end{pmatrix} \tag{24}$$

$$\begin{cases} q_{11} = \dfrac{1}{2\alpha^5}(1 - e^{-2\alpha T} + 2\alpha T + \dfrac{2\alpha^3 T^3}{3} \\ \qquad - 2\alpha^2 T^2 - 4\alpha T e^{-\alpha T}) \\ q_{12} = \dfrac{1}{2\alpha^4}(e^{-2\alpha T} + 1 - 2e^{-\alpha T} + 2\alpha T e^{-\alpha T} \\ \qquad - 2\alpha T + \alpha^2 T^2) \\ q_{13} = \dfrac{1}{2\alpha^3}(1 - 2e^{-2\alpha T} - 2\alpha T e^{-\alpha T}) \\ q_{22} = \dfrac{1}{2\alpha^3}(4e^{-\alpha T} - 3 - e^{-2\alpha T} + 2\alpha T) \\ q_{23} = \dfrac{1}{2\alpha^2}(e^{-2\alpha T} + 1 - 2e^{-\alpha T}) \\ q_{33} = \dfrac{1}{2\alpha}(1 - e^{-2\alpha T}) \end{cases} \tag{25}$$

wherein T is the sample period.

The "current" model adopts the standard Kalman filter discrete algorithm, which is illustrated as below [41].

$$\hat{X}(k+1|k) = \Phi(k)\hat{X}(k|k) + U(k)\bar{a}(k) \tag{26}$$
$$P(k+1|k) = \Phi(k)P(k|k)\Phi^T(k) + Q(k) \tag{27}$$
$$S(k+1) = H(k)P(k+1|k)H^T(k) + R(k) \tag{28}$$
$$K(k+1) = P(k+1|k)H^T(k)S^{-1}(k+1) \tag{29}$$
$$P(k+1|k+1) = [I - K(k+1)H(k)]P(k+1|k) \tag{30}$$
$$r(k+1) = Z(k+1) - H(k)\hat{X}(k+1|k) \tag{31}$$
$$\hat{X}(k+1|k+1) = \hat{X}(k+1|k) + K(k+1)r(k+1) \tag{32}$$

The normal Kalman filter has the same discretization form with $\bar{a}(\mathrm{k}) = 0$.

IV. SIMULATIONS AND MOBILE ROBOT EXPERIMENTS

Simulations and experiments of implementing the adaptive Kalman filter and the normal Kalman filter in the CACC controller during communication loss are conducted to compare and validate their tracking performances. Simulations are based on the automotive model in Matlab/Simulink, and experiments are conducted in a mobile robot platoon. The platoon in simulations and experiments are composed of two vehicles, in which the following vehicle is able to validate the proposed control strategy. The parameters of the automotive simulations are illustrated in Table 3.

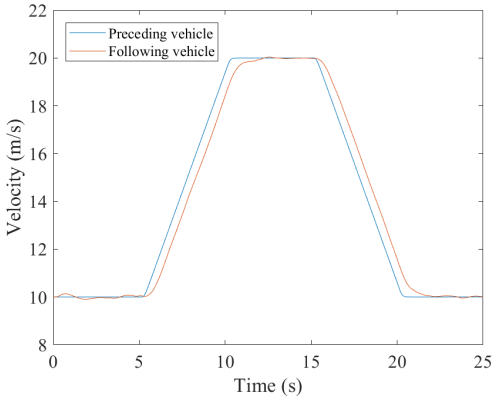

FIGURE 5. The velocity profile of automotive CACC (no communication loss).

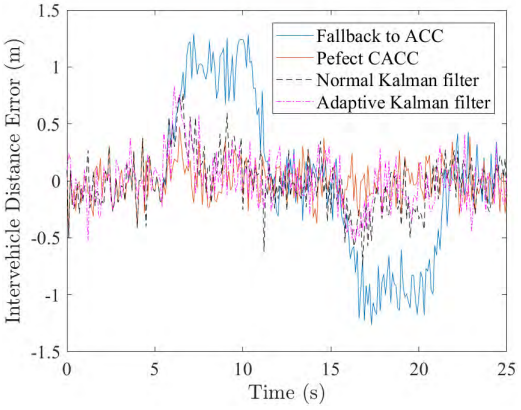

FIGURE 6. The inter-vehicle distance error in different strategies.

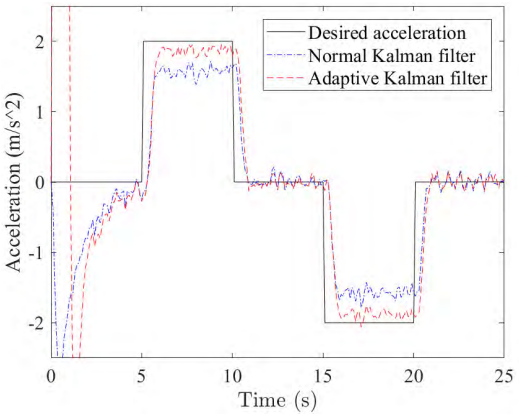

FIGURE 7. The estimated acceleration of the normal Kalman filter and the adaptive Kalman filter.

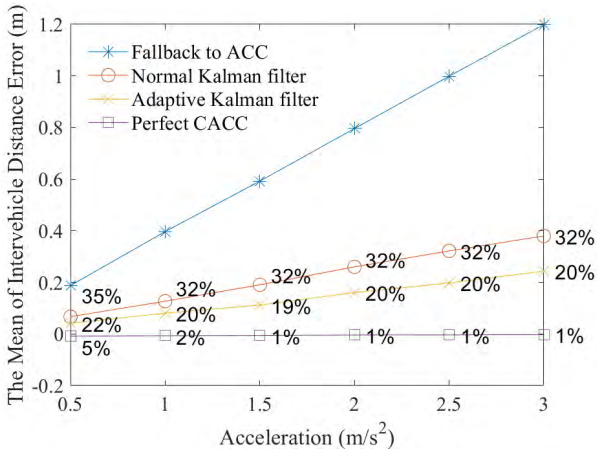

FIGURE 8. The mean of inter-vehicle distance error with different accelerations (The percentage means the corresponding mean divided by that for the fallback to ACC).

Mobile robots used in the experiments have the capability to emulate the vehicle platoon in real traffic [32]. Mobile robots are equipped with cameras, wireless cards, and infrared sensors. Each mobile robot has wireless communication, lane keeping, and inter-vehicle distance measurement capabilities. The lane keeping capability is based on the lane detection by cameras. The infrared sensors are used for the inter-vehicle distance measurement. The wireless communication code is developed by socket programming using UDP. The experimental platform is developed in [42]. More detailed settings of mobile robots are described in [32].

Four control strategies, including perfect CACC, CACC with the adaptive Kalman filter, CACC with the normal Kalman filter and fallback to ACC, are tested in simulations and experiments. As mentioned in Section I, the wireless communicated desired acceleration of preceding vehicle dominantly determines the total control action during the transient behavior. Hence, it's important to test these four control strategies during the acceleration and deceleration process. In simulations and experiments, communication loss is set to happen in the whole acceleration and deceleration process, and no communication loss happens in perfect CACC.

A. THE RESULTS OF REAL VEHICLE SIMULATIONS

In the vehicle (automotive) CACC simulations using a real vehicle model, there are two vehicles in the CACC platoon, and the velocity profile in perfect CACC (no communication loss) is demonstrated in Fig. 5. The vehicle model used in the simulations is based on equation (1) and its parameter is demonstrated in Table 3. The inter-vehicle distance errors of perfect CACC, CACC with the adaptive Kalman filter, CACC with the normal Kalman filter and fallback to ACC are displayed in Fig. 6. The estimated acceleration of the adaptive Kalman filter and the normal Kalman filter are illustrated by Fig. 7.

Five more velocity profiles of the preceding vehicle with different accelerations and decelerations (0.5, 1, 1.5, 2.5 and 3 m/s^2) are performed to validate the algorithms. The mean and RMS of inter-vehicle distance error during acceleration and deceleration are summarized in Fig. 8-11.

B. THE MOBILE ROBOT EXPERIMENTS SETUP

The mobile robot experiments are performed in a straight lane with white markers, as displayed in Fig. 12. The platoon has two mobile robots. Unlike radar, the infra-red sensor on

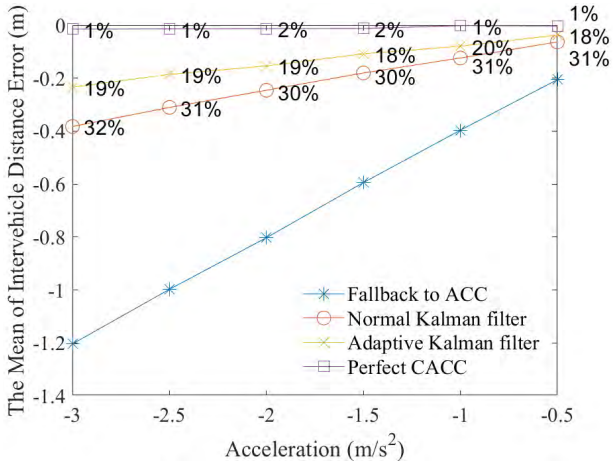

FIGURE 9. The mean of inter-vehicle distance error with different decelerations (The percentage means the corresponding mean divided by that for the fallback to ACC).

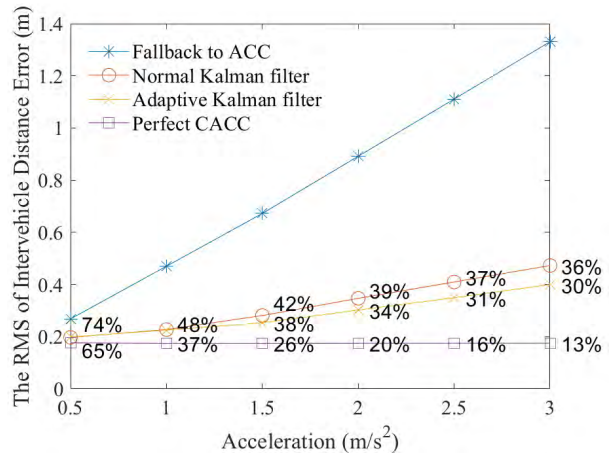

FIGURE 10. The RMS of inter-vehicle distance error with different accelerations (The percentage means the corresponding RMS divided by that for the fallback to ACC).

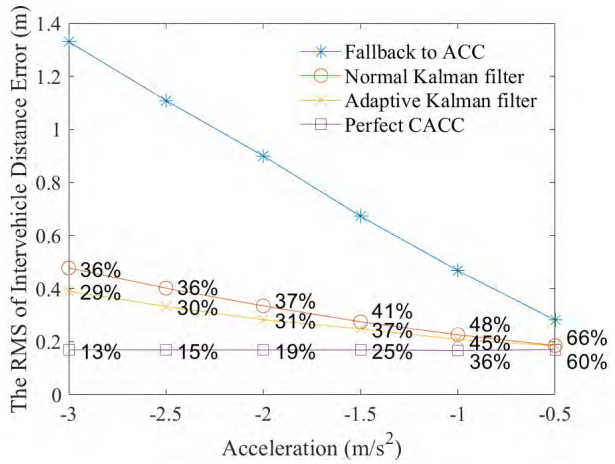

FIGURE 11. The RMS of inter-vehicle distance error with different decelerations (The percentage means the corresponding RMS divided by that for the fallback to ACC).

the mobile robot only can measure the inter-vehicle distance. Hence, a filtered version of relative velocity is implemented

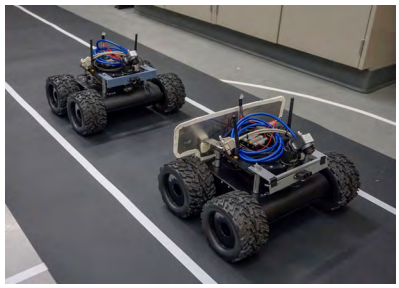

FIGURE 12. Mobile robot platoon experiments.

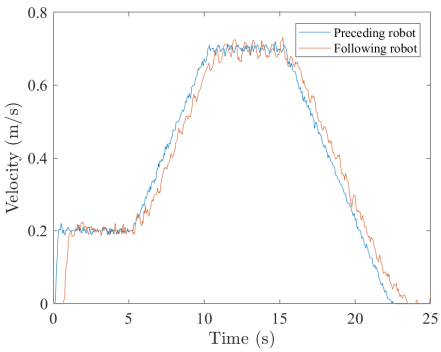

FIGURE 13. The velocity of mobile robots in perfect CACC (without communication loss).

for the measurement of relative velocity, as shown below. Furthermore, the robot velocity is measured by the wheel speed sensor in the electronic motor. And the robot position is estimated by the integration of the vehicle velocity, which is accurate enough for the robot running in a straight lane.

$$v_i(s) = \frac{s}{1+\tau s} q_i(s), \quad \tau \ll 1 \tag{33}$$

wherein $\triangle q_i(s)$ and $\triangle v_i(s)$ are the inter-vehicle distance and the relative velocity between vehicle i and vehicle $i-1$ in Laplace domain, respectively; and τ is a parameter for this filter.

C. THE RESULTS OF MOBILE ROBOT EXPERIMENTS

Two mobile robots form a CACC platoon for experiments. A desired velocity profile is designed in the preceding robot, as displayed in Fig. 13, and the following robot follows the preceding robot using the constant time gap policy. The velocity of the following robot in Fig. 13 is in perfect CACC. The acceleration and deceleration of the preceding robot are equal to 0.1 m/s^2.

The scenario of robot experiments is communication loss during acceleration (5-10s) and deceleration (15-22s). The inter-vehicle distance errors of four control strategies are demonstrated in Fig. 14-18. The estimated acceleration of the adaptive Kalman filter and the normal Kalman filter are illustrated by Fig. 19.

Two more velocity profiles of the preceding robot with different accelerations and decelerations (0.06 m/s^2 and 0.08 m/s^2) are performed to validate the algorithms. Also,

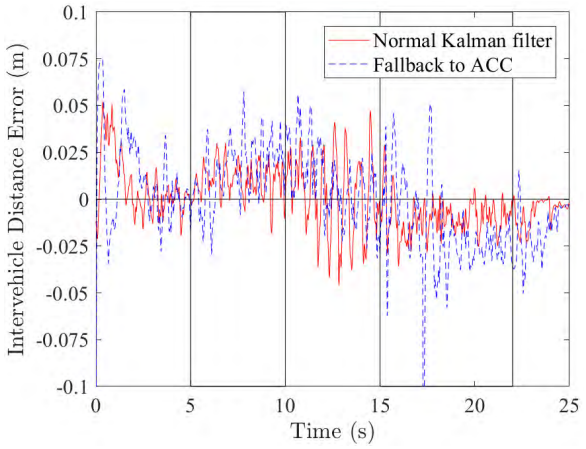

FIGURE 14. The inter-vehicle distance error of implementing the normal Kalman filter and falling back to ACC during communication loss.

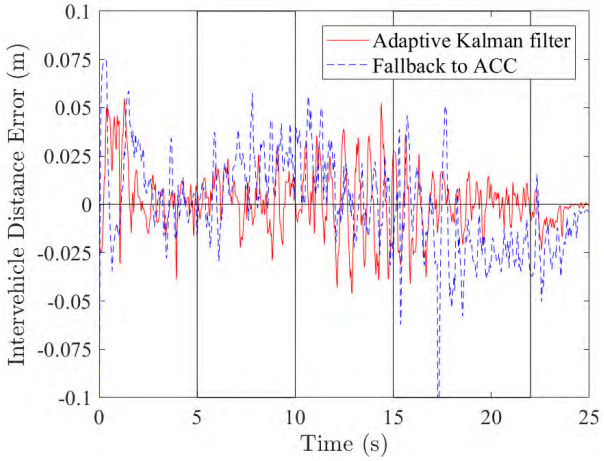

FIGURE 15. The inter-vehicle distance error of implementing the adaptive Kalman filter and falling back to ACC during communication loss.

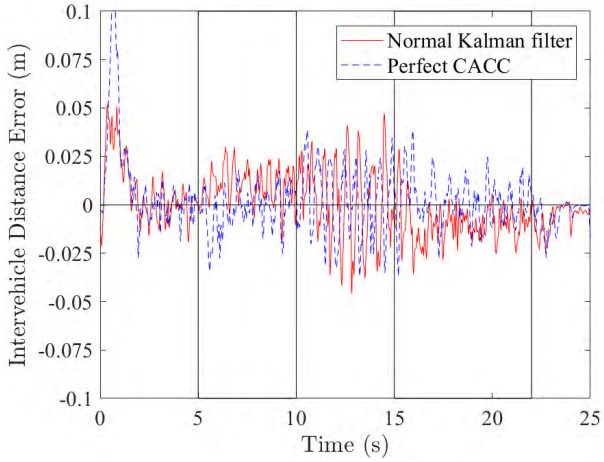

FIGURE 16. The inter-vehicle distance error of implementing the normal Kalman filter during communication loss and perfect CACC.

there is communication loss during the acceleration and deceleration process. The mean and RMS of inter-vehicle distance error during acceleration and deceleration are summarized in Fig. 20-23.

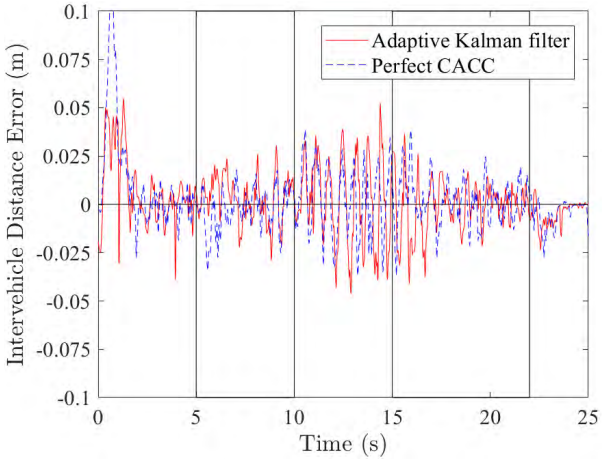

FIGURE 17. The inter-vehicle distance error of implementing the adaptive Kalman filter during communication loss and perfect CACC.

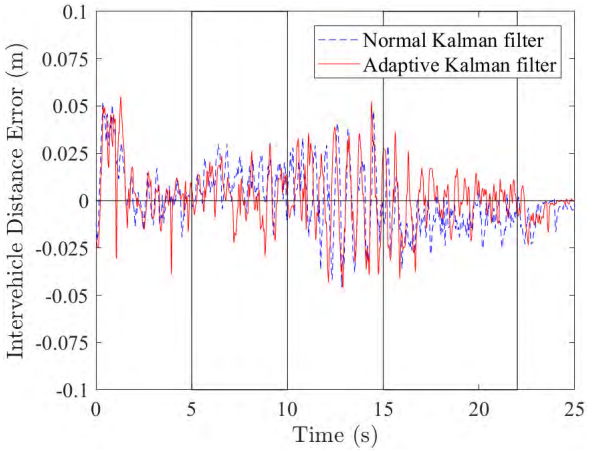

FIGURE 18. The inter-vehicle distance error of implementing the adaptive Kalman filter and the normal Kalman filter during communication loss.

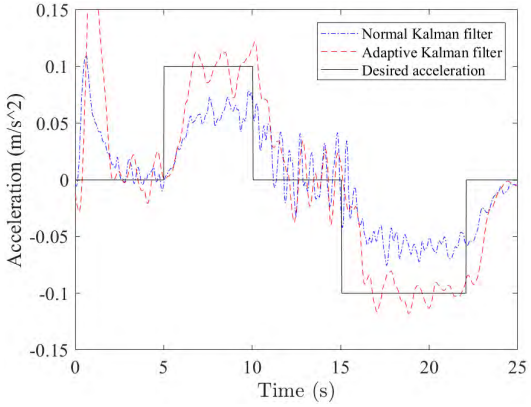

FIGURE 19. (Solid black) Desired acceleration, (dashed red) estimated acceleration in the adaptive Kalman filter and (dashed-dot blue) estimated acceleration in the normal Kalman filter.

D. RESULTS SUMMARIZATION AND ANALYSIS

The adaptive Kalman filter can estimate the longitudinal acceleration of the preceding vehicle accurately. And the acceleration estimation accuracy of the adaptive Kalman filter is better than the normal Kalman filter while they have

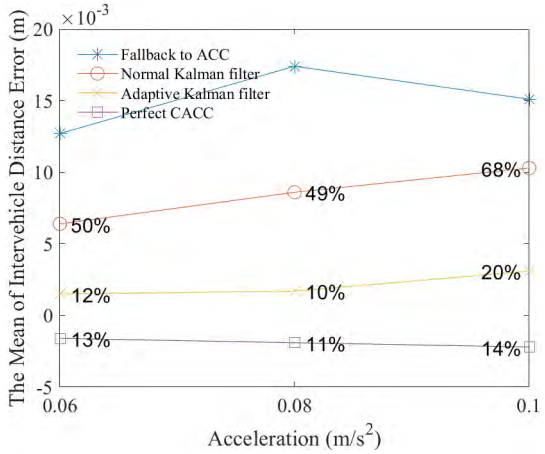

FIGURE 20. The mean of inter-vehicle distance error with different accelerations (The percentage means the corresponding mean divided by that for the fallback to ACC).

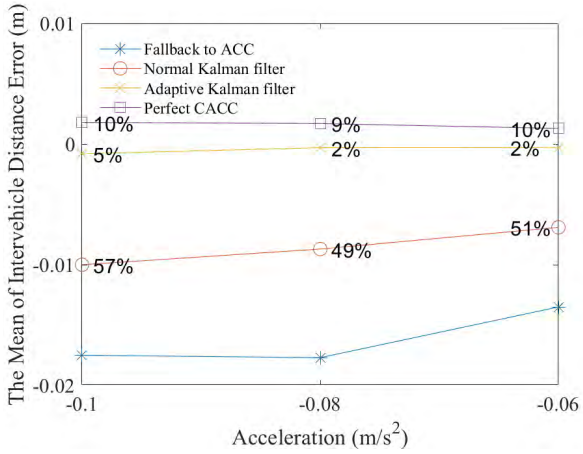

FIGURE 21. The mean of inter-vehicle distance error with different decelerations (The percentage means the corresponding mean divided by that for the fallback to ACC).

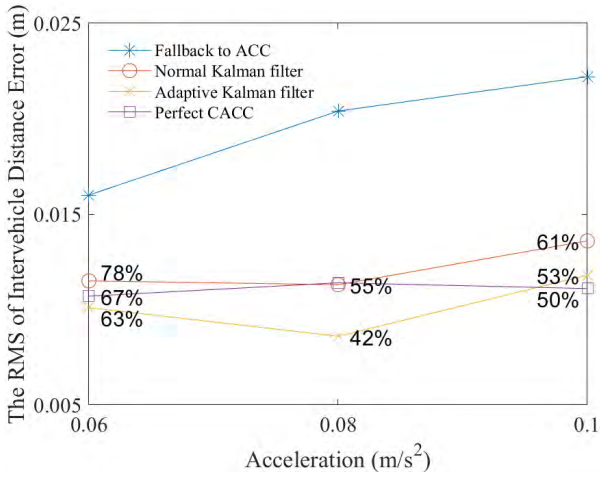

FIGURE 22. The RMS of inter-vehicle distance error with different accelerations (The percentage means the corresponding RMS divided by that for the fallback to ACC).

a similar convergence speed. In real vehicle simulations, as shown in Fig. 7, the estimated acceleration of the adaptive

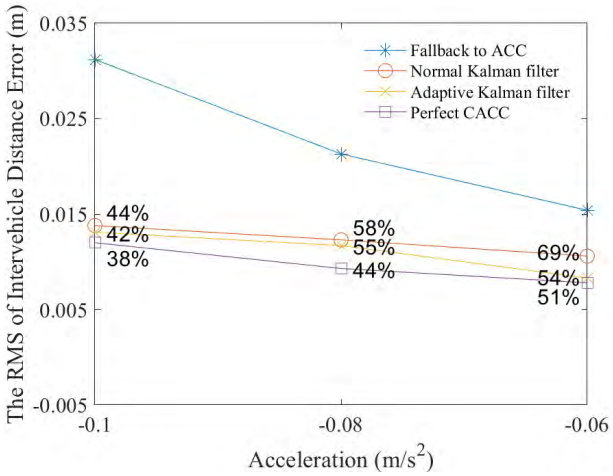

FIGURE 23. The RMS of inter-vehicle distance error with different decelerations (The percentage means the corresponding RMS divided by that for the fallback to ACC).

TABLE 1. Mobile robot experiments: The mean and RMS of inter-vehicle distance error.

Acceleration (m/s^2)	Mean			RMS		
	NKF	AKF	PCACC	NKF	AKF	PCACC
0.6	50%	12%	13%	78%	63%	67%
0.8	49%	10%	11%	55%	42%	55%
1	68%	20%	14%	61%	53%	50%
-0.6	51%	2%	10%	69%	54%	38%
-0.8	49%	2%	9%	58%	55%	44%
-1	57%	5%	10%	44%	42%	51%

The percentage means the corresponding mean or RMS divided by that for the fallback to ACC.

NKF: normal Kalman filter; AKF: adaptive Kalman filter; PCACC: perfect CACC.

Kalman filter is 92.5% of the desired acceleration, and the normal Kalman filter is 77.5%. And the convergence time of these two filters is around 0.8 second. In mobile robot experiments, as shown in Fig. 19, the estimated acceleration in the adaptive Kalman filter is 90-95% of the desired acceleration, and the estimated acceleration in the normal Kalman filter is 60-65% of the desired acceleration. And the convergence time of these two filters is around 1.35 second.

The mean of the inter-vehicle distance error in CACC with the adaptive Kalman filter is much less than fallback to ACC, which also has a substantial improvement, compared to CACC with the normal Kalman filter. In real vehicle simulations, as shown in Table 2, the mean of the inter-vehicle distance error in CACC with the adaptive Kalman filter is about 20% of fallback to ACC, and CACC with the normal Kalman filter is about 32%. In mobile robot experiments, as shown in Table 1, the mean of the inter-vehicle distance error in CACC with the adaptive Kalman filter is about 2-20% of fallback to ACC, and CACC with the normal Kalman filter is about 49-68%. The feedforward term in CACC controller, the desired acceleration of the preceding vehicle, is able to make the control error converge to zero faster. Hence, a more accurate estimation of the preceding vehicle's acceleration

TABLE 2. Real vehicle simulations: The mean and RMS of inter-vehicle distance error.

Acceleration (m/s^2)	Mean			RMS		
	NKF	AKF	PCACC	NKF	AKF	PCACC
0.5	35%	22%	5%	74%	74%	65%
1	32%	20%	2%	48%	48%	37%
1.5	32%	19%	1%	42%	38%	26%
2	32%	20%	1%	39%	34%	20%
2.5	32%	20%	1%	37%	31%	16%
3	32%	20%	1%	36%	30%	13%
-0.5	31%	18%	1%	66%	66%	60%
-1	31%	20%	1%	48%	45%	36%
-1.5	30%	18%	2%	41%	37%	25%
-2	30%	19%	2%	37%	31%	19%
-2.5	31%	19%	1%	36%	30%	15%
-3	32%	19%	1%	36%	29%	13%

The percentage means the corresponding mean or RMS divided by that for the fallback to ACC.

NKF: normal Kalman filter; AKF: adaptive Kalman filter; PCACC: perfect CACC.

leads to a smaller mean of the inter-vehicle distance error in case of communication loss.

The RMS of the inter-vehicle distance error in CACC with the adaptive Kalman filter is much less than fallback to ACC, and the difference between them is increasing with increasing acceleration. It also has a few reductions, compared to CACC with the normal Kalman filter. In real vehicle simulations, as shown in Table 2, the RMS of the inter-vehicle distance error in CACC with the adaptive Kalman filter is about 29-74% of fallback to ACC, and CACC with the normal Kalman filter is about 36-74%. In mobile robot experiments, as shown in Table 1, the RMS of the inter-vehicle distance error in CACC with the adaptive Kalman filter is about 42-63% of fallback to ACC, and CACC with the normal Kalman filter is about 44-78%.

V. CONCLUSION

The innovative CACC control strategy proposed in this paper effectively improve the performance of CACC during extended communication loss. The adaptive Kalman filter, based on the ''current'' model, can estimate the acceleration of the preceding vehicle and improve the performances of CACC during communication loss, which reduces the mean and RMS of inter-vehicle distance error significantly, compared to fallback to ACC. In the simulations and experiments, the results show the mean of inter-vehicle distance error in the adaptive Kalman filter is less than the normal Kalman filter based on the Singer model. Hence, implementing the adaptive Kalman filter is a better solution than the normal Kalman filter during communication loss.

Although the mobile robots emulating real vehicles provided a good initial proof of this concept and insights, in the future, real vehicle experiments need to be conducted to verify the implementation of the adaptive Kalman filter in CACC. Also, the platooning issues of multiple vehicles, like platoon stability analysis with or without communications loss and other communications related issues, need to be further studied in the future.

APPENDIX

TABLE 3. The parameters of automotive simulations.

Parameters	Description	Value
η_i	Vehicle actuator dynamic parameter	0.1s
$\tau_{a,i}$	Vehicle actuation delay	0.2s
h	Time gap	0.5s
r_i	Standstill distance	3m
k_p	PD controller coefficient	2
k_d	PD controller coefficient	2
θ	Wireless communication time delay constant	0.02s
α	Maneuvering frequency	$1.25s^{-1}$
P_0	Probability of zero acceleration	0.1
$P_{\max}$	Probability of maximum acceleration	0.01
$a_{\max}$	Maximum acceleration	$8m/s^2$
$\sigma^2_{\Delta d}$	Variance of measured inter-vehicle distance	$0.029m^2$
$\sigma^2_{\Delta v}$	Variance of measured relative vehicle velocity	$0.017m^2/s^2$

ACKNOWLEDGMENT

The authors would like to the Hubei Key Laboratory of Advanced Technology for Automotive Components, Hubei Collaborative Innovation Centre for Automotive Components Technology and Prof. Xuexun Guo from Wuhan University of Technology.

REFERENCES

[1] J. J. Blum, A. Tararakin, and A. Eskandarian, ''Efficient certificate distribution for vehicle heartbeat messages,'' in *Proc. IEEE 68th Veh. Technol. Conf.*, Sep. 2008, pp. 1–5.

[2] K. C. Dey, L. Yan, X. Wang, Y. Wang, H. Shen, M. Chowdhury, L. Yu, C. Qiu, and V. Soundararaj, ''A review of communication, driver characteristics, and controls aspects of cooperative adaptive cruise control (CACC),'' *IEEE Trans. Intell. Transp. Syst.*, vol. 17, no. 2, pp. 491–509, Feb. 2016.

[3] B. van Arem, C. J. G. van Driel, and R. Visser, ''The impact of cooperative adaptive cruise control on traffic-flow characteristics,'' *IEEE Trans. Intell. Transp. Syst.*, vol. 7, no. 4, pp. 429–436, Dec. 2006.

[4] B. B. Park, K. Malakorn, and J. Lee, ''Quantifying benefits of cooperative adaptive cruise control towards sustainable transportation system,'' Center Transp. Stud., Univ. Virginia, Charlottesville, VA, USA, Tech. Rep., 2011.

[5] G. J. L. Naus, R. P. A. Vugts, J. Ploeg, M. J. G. van de Molengraft, and M. Steinbuch, ''String-stable CACC design and experimental validation: A frequency-domain approach,'' *IEEE Trans. Veh. Technol.*, vol. 59, no. 9, pp. 4268–4279, Nov. 2010.

[6] S. E. Shladover, C. Nowakowski, X.-Y. Lu, and R. Ferlis, ''Cooperative adaptive cruise control: Definitions and operating concepts,'' *Transp. Res. Rec., J. Transp. Res. Board*, vol. 2489, no. 1, pp. 145–152, 2015.

[7] J. Ploeg, B. T. M. Scheepers, E. van Nunen, N. van de Wouw, and H. Nijmeijer, ''Design and experimental evaluation of cooperative adaptive cruise control,'' in *Proc. 14th Int. IEEE Conf. Intell. Transp. Syst. (ITSC)*, Oct. 2011, pp. 260–265.

[8] J. Ploeg, D. P. Shukla, N. van de Wouw, and H. Nijmeijer, ''Controller synthesis for string stability of vehicle platoons,'' *IEEE Trans. Intell. Transp. Syst.*, vol. 15, no. 2, pp. 854–865, Apr. 2014.

[9] K. Lidström, K. Sjoberg, U. Holmberg, J. Andersson, F. Bergh, M. Bjade, and S. Mak, ''A modular CACC system integration and design,'' *IEEE Trans. Intell. Transp. Syst.*, vol. 13, no. 3, pp. 1050–1061, Sep. 2012.

[10] E. van Nunen, J. Verhaegh, E. Silvas, E. Semsar-Kazerooni, and N. van de Wouw, ''Robust model predictive cooperative adaptive cruise control subject to V2V impairments,'' in *Proc. IEEE 20th Int. Conf. Intell. Transp. Syst. (ITSC)*, Oct. 2017, pp. 1–8.

[11] E. van Nunen, J. Ploeg, A. M. Medina, and H. Nijmeijer, "Fault tolerancy in cooperative adaptive cruise control," in *Proc. 16th Int. IEEE Conf. Intell. Transp. Syst. (ITSC)*, Oct. 2013, pp. 1184–1189.
[12] J. Ploeg, E. Semsar-Kazerooni, G. Lijster, N. van de Wouw, and H. Nijmeijer, "Graceful degradation of cooperative adaptive cruise control," *IEEE Trans. Intell. Transp. Syst.*, vol. 16, no. 1, pp. 488–497, Feb. 2015.
[13] J. J. Blum and A. Eskandarian, "Avoiding timeslot boundary synchronization for multihop message broadcast in vehicular networks," in *Proc. IEEE 69th Veh. Technol. Conf. (VTC)*, Apr. 2009, pp. 1–5.
[14] J. J. Blum, R. Natarajan, and A. Eskandarian, "Synchronization challenges in media access coordination for vehicular ad hoc networks," *Wireless Commun. Mobile Comput.*, vol. 11, no. 7, pp. 954–963, 2011.
[15] J. J. Blum and A. Eskandarian, "Adaptive space division multiplexing: An improved link layer protocol for inter-vehicle communications," in *Proc. IEEE Intell. Transp. Syst.*, Sep. 2005, pp. 455–460.
[16] J. J. Blum, A. Neiswender, and A. Eskandarian, "Denial of service attacks on inter-vehicle communication networks," in *Proc. 11th Int. IEEE Conf. Intell. Transp. Syst.*, Oct. 2008, pp. 797–802.
[17] J. Blum and A. Eskandarian, "CARAVAN: A communications architecture for reliable adaptive vehicular adhoc networks," SAE Tech. Paper 2006-01-1427, 2006.
[18] S. Santini, A. Salvi, A. S. Valente, A. Pescapé, M. Segata, and R. L. Cigno, "A consensus-based approach for platooning with intervehicular communications and its validation in realistic scenarios," *IEEE Trans. Veh. Technol.*, vol. 66, no. 3, pp. 1985–1999, Mar. 2017.
[19] D. Jia and D. Ngoduy, "Platoon based cooperative driving model with consideration of realistic inter-vehicle communication," *Transp. Res. C*, vol. 68, pp. 245–264, Sep. 2016.
[20] M. di Bernardo, A. Salvi, and S. Santini, "Distributed consensus strategy for platooning of vehicles in the presence of time-varying heterogeneous communication delays," *IEEE Trans. Intell. Transp. Syst.*, vol. 16, no. 1, pp. 102–112, Feb. 2015.
[21] Y. A. Harfouch, S. Yuan, and S. Baldi, "An adaptive switched control approach to heterogeneous platooning with intervehicle communication losses," *IEEE Trans. Control Netw. Syst.*, vol. 5, no. 3, pp. 1434–1444, Sep. 2018.
[22] K. K. Lee and S. T. Chanson, "Packet loss probability for real-time wireless communications," *IEEE Trans. Veh. Technol.*, vol. 51, no. 6, pp. 1569–1575, Nov. 2002.
[23] X. Liu, A. Goldsmith, S. S. Mahal, and J. K. Hedrick, "Effects of communication delay on string stability in vehicle platoons," in *Proc. IEEE Intell. Transp. Syst. (ITSC)*, Aug. 2001, pp. 625–630.
[24] W. B. Dunbar and D. S. Caveney, "Distributed receding horizon control of vehicle platoons: Stability and string stability," *IEEE Trans. Autom. Control*, vol. 57, no. 3, pp. 620–633, Mar. 2012.
[25] X. R. Li and V. P. Jilkov, "Survey of maneuvering target tracking. Part I. Dynamic models," *IEEE Trans. Aerosp. Electron. Syst.*, vol. 39, no. 4, pp. 1333–1364, Oct. 2003.
[26] A. Polychronopoulos, M. Tsogas, A. J. Amditis, and L. Andreone, "Sensor fusion for predicting vehicles' path for collision avoidance systems," *IEEE Trans. Intell. Transp. Syst.*, vol. 8, no. 3, pp. 549–562, Sep. 2007.
[27] J. Hillenbrand, A. M. Spieker, and K. Kroschel, "A multilevel collision mitigation approach—Its situation assessment, decision making, and performance tradeoffs," *IEEE Trans. Intell. Transp. Syst.*, vol. 7, no. 4, pp. 528–540, Dec. 2006.
[28] K. S. P. Kumar and H. Zhou, "A 'current' statistical model and adaptive algorithm for estimating maneuvering targets," *J. Guid. Control Dyn.*, vol. 7, no. 5, pp. 596–602, 1984.
[29] S. Öncü, J. Ploeg, N. van de Wouw, and H. Nijmeijer, "Cooperative adaptive cruise control: Network-aware analysis of string stability," *IEEE Trans. Intell. Transp. Syst.*, vol. 15, no. 4, pp. 1527–1537, Aug. 2014.
[30] S. E. Li, Y. Zheng, K. Li, Y. Wu, J. K. Hedrick, F. Gao, and H. Zhang, "Dynamical modeling and distributed control of connected and automated vehicles: Challenges and opportunities," *IEEE Intell. Transp. Syst. Mag.*, vol. 9, no. 3, pp. 46–58, Jul. 2017.
[31] J. Ploeg, N. van de Wouw, and H. Nijmeijer, "Fault tolerance of cooperative vehicle platoons subject to communication delay," *IFAC-PapersOnLine*, vol. 48, no. 12, pp. 352–357, 2015.
[32] Y. Lin and A. Eskandarian, "Experimental evaluation of cooperative adaptive cruise control with autonomous mobile robots," in *Proc. IEEE Conf. Control Technol. Appl. (CCTA)*, Aug. 2017, pp. 281–286.
[33] R. A. Singer, "Estimating optimal tracking filter performance for manned maneuvering targets," *IEEE Trans. Aerosp. Electron. Syst.*, vol. AES-6, no. 4, pp. 473–483, Jul. 1970.
[34] F. L. Lewis, D. L. Vrabie, and V. L. Syrmos, *Optimal Control*. Hoboken, NJ, USA: Wiley, 2012.
[35] M. Tanelli, S. M. Savaresi, and C. Cantoni, "Longitudinal vehicle speed estimation for traction and braking control systems," in *Proc. IEEE Conf. Comput. Aided Control Syst. Design, IEEE Int. Conf. Control Appl., IEEE Int. Symp. Intell. Control*, Oct. 2006, pp. 2790–2795.
[36] A. Eskandarian, *Handbook of Intelligent Vehicles*. London, U.K.: Springer, 2012.
[37] J. Degerman, K. Alenljung, and Y. Abe, "Simultaneous localization and mapping (SLAM) for automotive using forward looking radar," in *Proc. 3rd Int. Symp. Future Act. Saf. Technol. Toward Zero Traffic Accidents FAST-Zero*, 2015, pp. 258–265.
[38] N. Magnusson and T. Odenman, "Improving absolute position estimates of an automotive vehicle using GPS in sensor fusion," M.S. thesis, Dept. Signals Syst., Chalmers Univ. Technol., Göteborg, Sweden, 2012.
[39] W. Sun and Y. Yang, "Adaptive maneuvering frequency method of current statistical model," *IEEE/CAA J. Automatica Sinica*, vol. 4, no. 1, pp. 154–160, Jan. 2017.
[40] H. You, X. Jianjuan, and G. Xin, *Radar Data Processing With Applications*. Hoboken, NJ, USA: Wiley, 2016.
[41] H. Shi, D. Zhou, and C. Chen, "A novel adaptive filtering algorithm for maneuvering target tracking," in *Proc. Int. Symp. Instrum. Meas., Sensor Netw. Automat. (IMSNA)*, Aug. 2012, pp. 209–213.
[42] Y. Lin, C. Wu, and A. Eskandarian, "Integrating odometry and intervehicular communication for adaptive cruise control with target detection loss," in *Proc. IEEE Intell. Vehicles Symp. (IV)*, Jun. 2018, pp. 1848–1853.

CHAOXIAN WU received the B.S. degree in vehicle engineering from the Wuhan University of Technology, China, in 2014, where he is currently pursuing the Ph.D. degree in vehicle engineering. He is also a Visiting Ph.D. Student with the Department of Mechanical Engineering, Virginia Tech, Blacksburg, VA, USA. His research interests include mechatronics design, vehicle brake systems, vehicle dynamics and control, and autonomous vehicle.

YUAN LIN received the B.E. degree in civil engineering from Nanchang University, China, in 2011, and the Ph.D. degree in engineering mechanics from Virginia Tech, Blacksburg, VA, USA, in 2016. He started to work as a Postdoctoral Research Associate at the Autonomous Systems and Intelligent Machines Laboratory, Mechanical Engineering Department, Virginia Tech. His research interests include robotics, control, sensor fusion, and V2X.

AZIM ESKANDARIAN received the B.S. degree from George Washington University (GWU), the M.S. degree from Virginia Tech, and the D.Sc. degree from GWU, all in mechanical engineering.

He was a Professor of engineering and applied science with GWU and the Founding Director of the Center for Intelligent Systems Research, from 1996 to 2015, the Director of the Transportation Safety and Security University Area of Excellence, from 2002 to 2015, and the Co-Founder of the National Crash Analysis Center, in 1992 and the Director of the National Crash Analysis Center, from 1998 to 2002 and 2013 to 2015. He was an Assistant Professor with Pennsylvania State University, York, PA, USA, from 1989 to 1992, and an Engineer/Project Manager in industry, from 1983 to 1989. He has been a Professor and the Head of the Mechanical Engineering Department, Virginia Tech (VT), since 2015. He became the Nicholas and Rebecca Des Champs Chaired Professor, in 2018. He established the Autonomous Systems and Intelligent Machines Laboratory at VT to conduct the research in intelligent and autonomous vehicles, and mobile robotics.

Dr. Eskandarian is a Fellow of ASME and a member of SAE professional societies. He received the IEEE ITS Society's Outstanding Researcher Award, in 2017, and the GWU's School of Engineering Outstanding Researcher Award, in 2013.